THE EFFECT OF DIFFERENT SURFACE COATINGS ON THE $LiMn_2O_4$/MWCNT NANOCOMPOSITE CATHODES FOR IMPROVED ENERGY STORAGE CAPACITY

A. Akbulut[1*], M.O. Guler[2], H. Akbulut[2], I, A. Sengil[1]

[1]*Sakarya University, Engineering Faculty, Dept. of Environmental Engineering, Esentepe Campus, 54187, Sakarya, TURKEY*
[2]*Sakarya University, Engineering Faculty, Dept. of Metallurgy and Materials Engineering, Esentepe Campus, 54187, Sakarya, TURKEY*
**akbulutahsen@gmail.com*

Keywords: Li-ion batteries, $LiMn_2O_4$/MWCNT nanocomposite, SEI.

Abstract
In this study, it is aimed to develop $LiMn_2O_4$/MWCNT nanocomposites and electrode surface coating by Au-Pd, ZnO and SiO_2 to overcome poor conductivity and decomposition in the electrolyte during charging and discharging. The nanocomposites were produced by sol–gel method, which allows producing very fine particle size of $LiMn_2O_4$ free from Mn_2O_3 at the low temperature of 300 ^oC. Coin-type (CR2016) test cells were assembled, directly using the $LiMn_2O_4$, $LiMn_2O_4$/MWCNTs and surface coated $LiMn_2O_4$/MWCNTs, a lithium metal foil as the counter electrode. Nanocomposites of $LiMn_2O_4$/MWCNT with surface coating with Au-Pd and ZnO show high cycle performance with a remarkable capacity retention even at long cycles. Impedance measurements show that the charge-transfer resistance of the nanocomposites with their surfaces was coated is lower than that of spinel $LiMn_2O_4$.

1 Introduction
Currently, $LiCoO_2$, $LiNiO_2$, $LiMn_2O_4$ and $LiFePO_4$ have been widely investigated for Li-ion batteries (LIBs) with large energy capacity and power density, and good cycling stability. Among the four, $LiMn_2O_4$ is a promising material to be used in new-generation commercial LIBs due to its unique advantages of low cost, abundant resource, nontoxicity, environmental safety, easy preparation, and being environmentally friendly [1, 2]. Despite the advantages, there are limiting factors to use $LiMn_2O_4$ batteries in EV and other high-energy applications. The capacity fading result from: (I) Dissolution of Mn^{2+}, (II) Jahn-Teller distortion and (III) decomposition of electrolyte solution on the electrode. Particularly, dissolution of Mn^{2+} is considered an obstacle to its commercialization. To address this, numerous methods have been developed to fabricate highly-crystalline, nanostructured $LiMn_2O_4$ that serves to improve the structural stability and the cycling ability by shielding Mn^{2+} from dissolution to the electrolyte and volume expansion [3]. Hence, a group of methods has been proposed to eliminate these problems. The first proposed method is doping different cations, such as Al, Ga, Co, Cr, Ti into spinel $LiMn_2O_4$ in order to improve its structural stability [1, 4, 5]. However, $LiMn_2O_4$ still suffers from capacity fading at room and elevated temperatures due to Mn^{3+} dissolution, which occurred in the interface between the electrode and electrolyte during charge–discharge process [1,4,6]. Second proposed method is surface modification of

the cathode. Coating with metal oxides and stable pure metals seems more effective way to overcome this problem. Several surface metal oxides such as MgO, Al_2O_3, TiO_2, ZrO_2, ZnO and $Li_2O.2B_2O_3$, ZnO, CeO_2, and gold have been investigated and excellent cyclability [7].

Multiwalled carbon nanotubes (MWCNTs) have unique one-dimensional tubular structure, high electrical conductivity and large surface area; have been considered an ideal nanomaterial to functionalize other materials for applications in energy conversion and storage. MWCNTs form a network. Therefore, electrical conductivity of the LiMn2O4 battery increase while decreasing the charging resistance. Hybrid nanostructures composed of MWCNTs, and active materials possess not only the inherent properties of nanocrystals and MWCNTs acting alone, but also additional, unique properties that arise from the electrical and thermal interactions between them [8].

In this study, it is aimed to develop of MWCNT/$LiMn_2O_4$ nanocomposites and electrode surface coating by ZnO, SiO_2 and Au-20 wt. % Pd to overcome poor conductivity and decomposition in the electrolyte during charging and discharging. Although there are studies applying cathode surface coating with metal oxide and gold, there is no comprehensive study to show both surface coating and MWCNTs reinforcement together to reveal the combined effect of hybrid nanocomposites structure and surface coatings.

2. Experiment Details

2.1 Electrode Preparation

The $LiMn_2O_4$ powders were produced by using a well-known sol-gel method at the low temperature to obtain very fine nanocrystalline structures, and citric acid were used for the process. At first, manganese acetate tetrahydrate, $Mn(CH_3COO)_2.4H_2O$ (99.999%, Sigma–Aldrich),was dissolved in 50 ml distilled water. Lithium acetate dehydrate, $LiCH_3COO.2H_2O$ (99.999%, Sigma–Aldrich), was then added with mild stirring. To this solution, citric acid was added as a chelating agent and ammonia to maintain pH between 7 and 10. Then the solution was heated with vigorous stirring to remove excess ammonia and water. The temperature was gradually increased from 60 ^oC to 90 ^oC while vigorous stirring was maintained until a transparent gel was obtained. The resultant gel was dried at 120 °C for 10 h and was calcined at 300 °C for 24 h in air. The nanocomposites of $LiMn_2O_4$ reinforced with 5.0 wt. % MWCNT was prepared by mechanical alloying. MWCNT and $LiMn_2O_4$ powder was placed in 80 ml stainless steel mixing jars containing steel milling balls of 10 mm diameter (giving an initial ball-to-powder weight ratio (BPR) = 15:1). The jars were agitated using a high energy planetary ball mill (Fritsch Pulverisette F7) at 500 rpm for milling time of 1 h. MWCNTs used for this work were purchased from Arry Nano Inc. They have purity higher than 95%, their outer diameter of 50 nm and their length between 1.0 and 50 μm.

For the preparation of electrodes, 70 wt. % $LiMn_2O_4$ or powders were mixed with 20 wt.% acetylene black (conducting agent), and 10 wt.% polyvinylidene floride (binder-PVDF). Excess 1-methyl-2- pyrrolidone (NMP) was then added until the slurry reached a suitable viscosity, and then the slurry was uniformly coated on an Al-foil to obtain 500 μm thicknesses. The electrode (ca. 4 mg active material) was dried at 80 °C for 4h and subsequently at 120 °C for 24 h. The surfaces of some selected bare cathodes and nanocomposites were coated with Au-Pd, ZnO and SiO_2 by magnetron sputtering method using magnetron sputtering PVD with thickness of 10 nm.

2.2 Characterization

A Rigaku (D/MAX/2200) X-ray diffraction (XRD) with a grazing incidence attachment and CuKα radiation was used. The diffraction patterns were registered in the step scan mode, with a beam incidence angle of 0.5°, and recorded at 2° (2θ) steps with a constant time of 1 min per step in the range 10° < 26 < 90°. Scanning electron microscopy (SEM) (Jeol 6060LV) has been used to determine morphologies of the nanocomposite electrodes. Thermogravimetric and differential thermal analysis (TG/DTA) of the obtained gel was performed with a TA instruments (SDT Q600) at a heating rate of 10 °C/min^{-1} in a constant flow of extra dry air between room temperature and 700 °C. Coin-type (CR2016) test cells were assembled in an argon-filled glove box, directly using the $LiMn_2O_4$ and $LiMn_2O_4$/MWCNTs nanocomposites coated on Al foil as the working electrode, a lithium metal foil as the counter electrode, a micro porous polypropylene (PP) membrane (Cellgard 2300) as the separator, and 1M solution of $LiPF_6$ in ethylene carbonate (EC) and dimethyl carbonate (DMC) (1:1 by weight) as the electrolyte. The cells were cyclically tested on a MTI-BST8 battery tester using 1.0 C over a voltage range of 3.0-4.3 V. All tests were performed at room temperature (25 °C). The electrochemical impedance spectroscopy (EIS) was carried out by applying an ac voltage of 10 mV over the frequency range from 1Hz to 1000 kHz (Gamry Instrument Version 5.67).

3. Results and Discussions

3.1. XRD analysis

XRD analysis of all nanopowders, prepared as unreinforced active material (Fig. 1a), $LiMn_2O_4$/MWCNTs (Fig. 1b) and also bare MWCNTs (Fig.1c) are shown. All reflections for a synthesized $LiMn_2O_4$ perfectly match the LiMn2O4 lines corresponding JPDS card number of 35-0782. The XRD patterns for $LiMn_2O_4$ and its nanocomposite do not show significant differences and there are no characteristic C peaks, corresponding to MWCNTs since its content is not high to detect XRD. All the powders well defined spinel structure with a space group of Fd_3m in which the lithium ions occupy the tetrahedral 8a site whereas Mn^{3+} and Mn^{4+} ions reside at the octahedral 16d site and O^{2-} ions are located at the 32e site [9]. Lattice parameters calculated from the patterns from Fig. 1 are found to be 8.247 Å both for unreinforced $LiMn_2O_4$ and $LiMn_2O_4$/MWCNTs. Since the sol-gel process, we have applied eliminated Mn_2O_3 formation even at low sintering temperature of 300 °C, the XRD of both electrodes shown in Fig. 1 possess high peak broadening. The average dimension of crystallites d was estimated from the linewidths of XRD reflections by the Scherrer formula. It was calculated that grain sizes of $LiMn_2O_4$ and $LiMn_2O_4$/MWNCTs were found approximately 28.12 nm and 30.03 nm, respectively. It is well known that Scherrer's calculation does not taking into the consideration of the lattice strain and so, we have decided

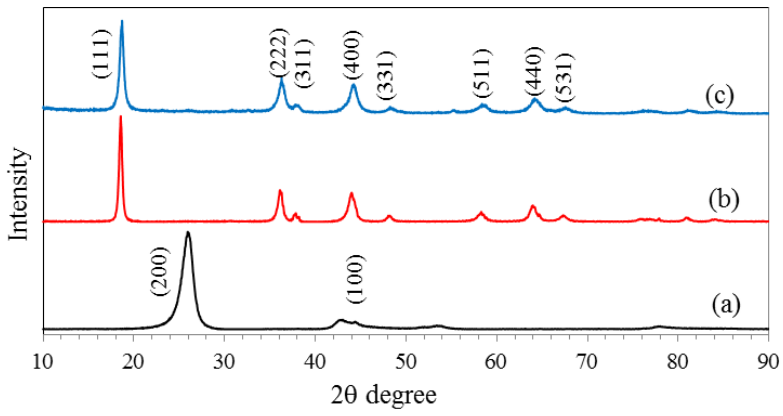

Figure 1. The XRD patterns of (a) MWCNTs b) bare $LiMn_2O_4$ and c) $LiMn_2O_4$/MWCNTs nanocomposite.

to calculate the Stoke's strain independently, in order to understand the effect of crystallite size and lattice strain on the $LiMn_2O_4$ and $LiMn_2O_4$/MWCNT nanocomposite electrodes. As also stated by Jayaprakash et al.[10], in nano sized coatings peak broadening is due to the finite crystallite size and not due to the instrumental effect or strain, based on the smaller Stoke's strain values. The calculated strain values are found higher in the MWCNT reinforced $LiMn_2O_4$ compared with bare $LiMn_2O_4$. For example, the lattice strain was calculated as 10.33 $x10^{-3}$ for $LiMn_2O_4$ electrode at (111) plane whereas in the $LiMn_2O_4$/MWCNT nanocomposite the strain value was calculated as 13.05 $x10^{-3}$ in the same plane.

Plane	$LiMn_2O_4$	$LiMn_2O_4$/MWCNT
(111)	10.33	13.04
(311)	7.6	8.90
(222)	6.0	8.02
(400)	7.3	7.55
(331)	5.5	7.01
(511)	5.1	6.60

Table 1. Lattice strain values for specific planes for $LiMn_2O_4$ and $LiMn_2O_4$/MWCNT sintered at 300 ^oC ($x10^{-3}$)

3.2. Microstructural characteristics

The surface morphology of $LiMn_2O_4$ and $LiMn_2O_4$/MWCNT electrodes were investigated. Fig. 2 presents SEM images of $LiMn_2O_4$ powders obtained from citric acid sol-gel process. In Fig. 2a, low magnification SEM micrograph is presented and show porous structure of the active material after sintering at 300 °C for 24 h. Fig. 2b presents high magnification micrograph of the same structure shown in Fig 2a. Since the microstructure of all the samples

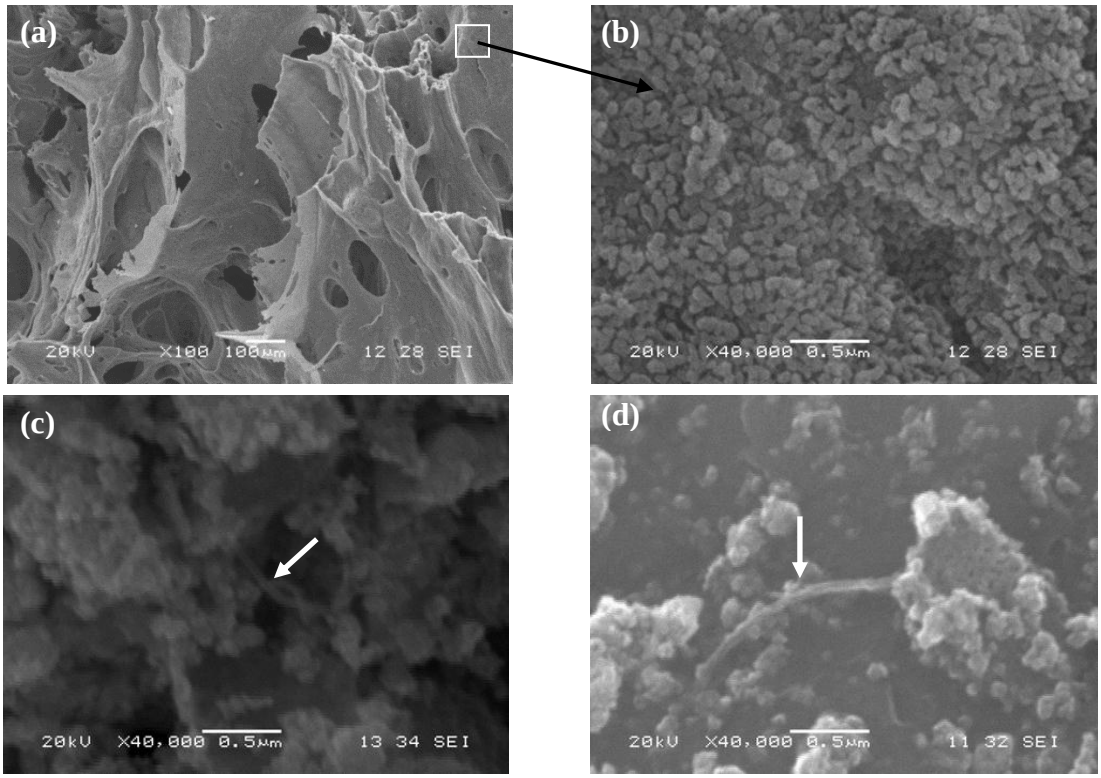

Figure 2. SEM photographs of (a) $LiMn_2O_4$ after sintering at low and (b) high magnification, c) $LiMn_2O_4$ after grinding and d) $LiMn_2O_4$ coated with Au-Pd after grinding.

after grinding is very similar to each other, regardless of the Au-Pd, ZnO and SiO_2 coating only the microstructures of uncoated and Au-Pd coated $LiMn_2O_4$ materials are shown in Fig. 2c and 2d, respectively. Since the amount of MWCNTs is only 5.0 wt. % and most of the MWCNTs were coated by the active materials during ball milling, it was experienced that observing MWCNTs it is difficult. In Fig. 2c and d, some detected MWCNTs are shown with arrows. EDS analysis was also proven that the marked species were MWCNTs.

3.3. Thermal Analysis

As we can see in fig.4, there is a remarkable weight loss between 150-320 °C. Weight loss begins approximately 150 °C is because of water evaporation. And weight loss proceeded because of decomposition of citric acid and acetate ions. Fig. 3 shows the TG–DTA curves for the thermal decomposition of the precursor $LiMn_2O_4$ prepared by the citric acid-based gel method. The TG curve displays four discrete weight-loss steps, and no more weight loss above 400 °C. Weight loss occurs in four temperature regions: 118–158, 158–230, 230-316, and 316–700 °C. The small weight loss of the first region may be attributed to superficial water loss due to the hygroscopic nature to the precursor complex. In the second region, the DTA curve shows one endothermic peak at 173 °C, which is attributed to the loss of chemically, bonded water in the sample. Third region is due to the decomposition of the inorganic and the organic constituents of precursor. In this region, the one exothermic peak observed at 295 °C is accompanied by noticeable weight loss in the TG curve. It is due to the decomposition of the inorganic, and the organic constituents of the precursor followed by crystallization of the $LiMn_2O_4$ phase. Increasing the temperature approximately beyond 320 °C results TG curve becomes flat and no sharp peaks can be observed on the DTA curve, indicating that no phase transformation occurs, and that any further heating only makes the structure of samples more crystalline.

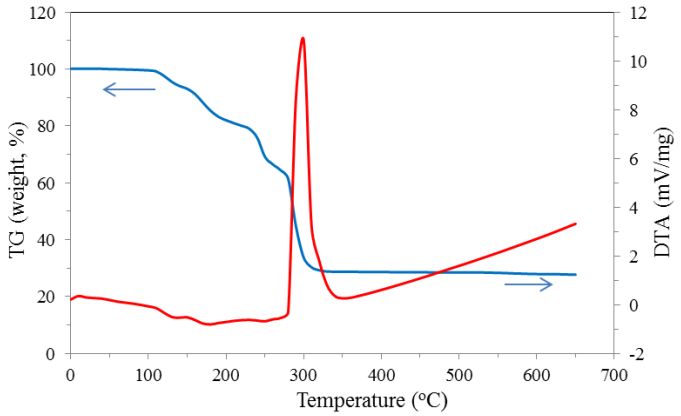

Figure 3. The TGA and DTA results of the dried $LiMn_2O_4$ precursor gel.

3.4. Electrochemical Results

Fig. 4 shows discharge capacities as a function of cycles for the as-prepared $LiMn_2O_4$, $LiMn_2O_4$/MWCNT and their Au-Pd, ZnO and SiO_2 coated electrodes at room temperature. In general, increasing cycle number resulted in decreasing discharge capacity. However, the initial capacities and the capacity fading rates show dissimilar characteristics depending on the MWCNT addition and coating with different materials. The bare $LiMn_2O_4$ shows fairly high initial capacity (108 $mAhg^{-1}$) but the cell performance exhibits very sharp decrease in capacity with increasing cycle number. Coating of $LiMn_2O_4$ electrode surface with ion sputtering yields high discharge capacities for the initial cycles and also prevented the decrease of capacity with increasing cycles. Therefore, it can be concluded that the electrodes coated with Au-Pd, ZnO and SiO_2 with 10 nm thickness has better cycling performance than

the uncoated one. Introducing 5.0 wt. % MWCNTs into $LiMn_2O_4$ results to increase both initial capacity and capacity retention with increasing cycle. All the nanocomposite electrodes reinforced with MWCNTs show nearly the same characteristics discharge capacities. However, Au-Pd coated nanocomposites showed highest discharge capacity and best capacity retention. For example, initial capacity of Au-Pd coated $LiMn_2O_4$/MWCNT nanocomposite yielded an initial capacity of 135.5 $mAhg^{-1}$ and showed 123 $mAhg^{-1}$ discharge capacities, which correspond approximately 92 % of its discharge capacity retention even at 100 cycles.

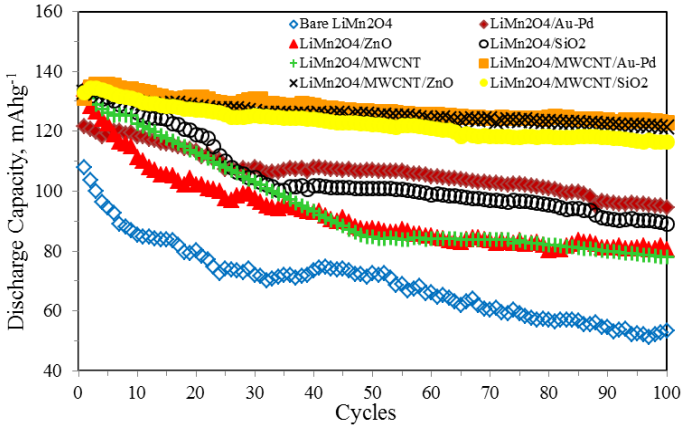

Figure 4. Discharge capacity versus cycle number for $LiMn_2O_4$ based nanocomposites electrodes.

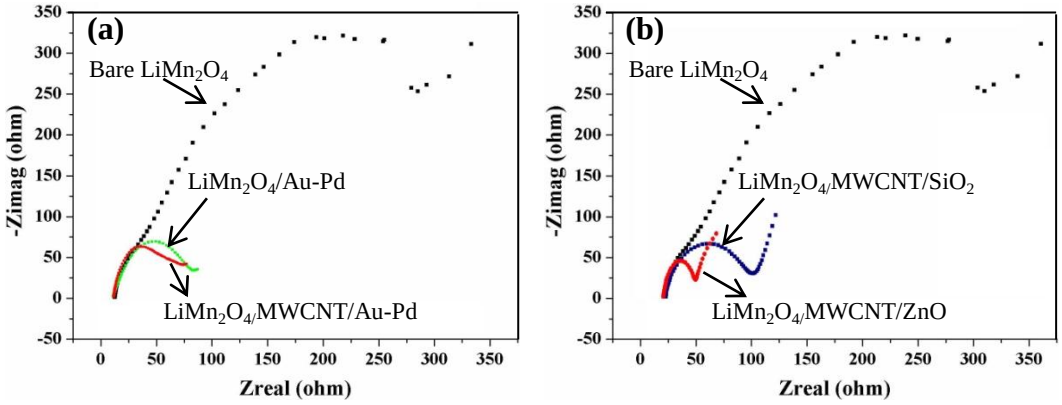

Figure 5. EIS spectra for (a) bare $LiMn_2O_4$, $LiMn_2O_4$/Au-Pd, $LiMn_2O_4$/MWCNT/Au-Pd and (b) bare $LiMn_2O_4$/, $LiMn_2O_4$/MWCNT/ZnO and $LiMn_2O_4$/MWCNT/SiO_2 nanocomposites

For evaluating further the electrochemical characteristics of $LiMn_2O_4$ and its nanocomposites, the electrochemical impedance spectroscopy (EIS) experiment was carried out, and the EIS graph was shown in Fig. 5 for some selected nanocomposites. It can be seen from Fig. 5 coatings of the $LiMn_2O_4$ electrode surfaces with a thin layer of 10 nm in thickness Au-Pd, ZnO and SiO_2 seems very effective to suppress reaction between $LiMn_2O_4$ and electrolyte. Additionally, introducing MWCNT into $LiMn_2O_4$ is also very beneficial to prevent SEI formation. It is well known that the semicircle corresponding to the passivation film formed by the reaction between the oxide and electrolyte [11]. The decrease of diameter of the semicircle is seen for all the coatings, and MWCNT added nanocomposites refer suppression of reactions. Literature about EIS reports that, a circle at the high-to-middle frequency semicircle represents the resistance for the Li-ions migration through the SEI layer and film capacitance, another semicircle at the low-frequency semicircle is related to charge transfer resistance and interfacial capacitance between the electrode and electrolyte interface, and the slopping straight line at very low frequency corresponds to the Li-ions diffusion in the bulk

materials, and the intercept of the high-frequency semicircle on the real axis (Zreal axis) represents resistance contribution coming from the electrolyte solution. It is clear from the Fig. 5a, and 5b that a pronounced difference appeared at the surface film of cathodes when MWCNTs were used as reinforcing component. In spite of higher lattice strain values in the case of MWCNT addition, both the discharge capacities and EIS results are obtained to be better in comparison with bare $LiMn_2O_4$. This is because of increased conductivity and amount of Li ions absorption emanated from MWCNTs [8]. The diameter of the low-frequency semicircle, representing charge transfer resistance, decreases from 282 to 61.5 Ω when coated with Au-Pd and introducing MWCNTs resulted in a decrease in the resistance to 52 Ω (Fig. 5a). In Fig. 5b, the EIS measurements of MWCNT/$LiMn_2O_4$ electrodes coated with ZnO, and SiO_2 are shown. Similar to the Au-Pd coating, remarkable decreases are seen in the charge transfer resistance. For example, in ZnO coated $LiMn_2O_4$/MWCNT electrode the resistance is measured as 55 Ω, whereas SiO_2 coated electrode produced 149 Ω.

From the EIS results, it can be concluded that MWCNT addition and coating the electrode surfaces with a 10 nm Au-Pd and ZnO provide very attractive results to prevent Mn dissolution into the electrolyte. However, SiO_2 coating seems also attractive method, although it produces higher resistance. As Wang et al. [12] reported, capacity loss caused by dissolution of Mn accounted on overall capacity loss at room temperature. Gold is known and found several applications to coat on the $LiMn_2O_4$ particle surfaces and caused to prevent Mn dissolution [13]. In our study, we have applied more practical method to coat the overall electrode surfaces of $LiMn_2O_4$/MWCNT with the thin layers of Au-Pd, and this method provided very good capacity retention and low resistance. Increasing cell potential in the case of ZnO and SiO_2 is thought because of different mechanisms. It can be speculated that the surface coating of ZnO suppressed the formation of passivation on the surface of the $LiMn_2O_4$, preventing the electrolyte decomposition which leads to the dissolution of the Mn ion. On the other hand, it may be easier for ZnO to dissolve into the electrolyte, so the Mn ion dissolution was reduced.

4. Conclusions

Citric acid sol-gel method was used to produce Mn_2O_3 free, crystalline and mesoporous $LiMn_2O_4$ electrodes at a low temperature of 300 ^oC. Although very fine grains of active material are suggested because of poor stability, our attractive results are given as follows:

1. Using citric acid sol-gel method with a continuous heating of the solution from 60 ^oC to 90 ^oC resulted in highly porous $LiMn_2O_4$ with nano grains between 28.12 nm and 30.03 nm.
2. Introducing MWCNTs into $LiMn_2O_4$ caused the lattice strain increase of approximately 20 % depending on the different crystallographic planes.
3. 5.0 wt. % MWCNT addition into $LiMn_2O_4$ increases discharge capacity of the $LiMn_2O_4$ from 53.3 $mAhg^{-1}$ to 78 $mAhg^{-1}$ after 100 cycles test.
4. Au-Pd, SiO_2 and ZnO coatings on $LiMn_2O_4$ with 10 nm thickness increased discharge capacity to 94.3 $mAhg^{-1}$, 89 $mAhg^{-1}$ and 80.5 $mAhg^{-1}$, respectively, after 100 cycles.
5. Introducing 5.0 wt. % MWCNTS into $LiMn_2O_4$ and then subsequent coating with Au-Pd, ZnO and SiO_2 yielded discharge capacities after 100 cycles electrochemical test produced discharge capacities of 122.8 $mAhg^{-1}$, 121,3 $mAhg^{-1}$ and 116,5 $mAhg^{-1}$, respectively.
6. Au-Pd coated $LiMn_2O_4$/MWCNT nanocomposite yielded an initial capacity of 135.5 $mAhg^{-1}$ and showed 123 $mAhg^{-1}$ discharge capacity, which corresponds approximately its discharge prevented approximately 92 % of its capacity even at 100 cycles.

7. EIS measurements showed that MWCNT addition and electrode surface coating provides charge transfer resistance, decreases of $LiMn_2O_4$ from 282 to 61.5 Ω when coated with 10 nm Au-Pd and introducing MWCNTs resulted in a decrease in the resistance to 52 Ω.

Acknowledgements
The authors thank the Scientific and Technological Research Council of Turkey (TUBITAK) for their financial support under the contract number of 111M021.

References

[1] Guan D., Cai C., Wang Y., Enhanced cycleability of $LiMn_2O_4$ cathodes by atomic layer deposition of Al_2O_3 Coatings, *Nanoscale*, **3**, 1465-1469, (2011).
[2] Liu Y.J., Guo H.J., Li X.H., Wang Z.X., Study on the storage performance of manganese spinel battery, *Advanced Mater. Research*, **347-353**, 1395-1398, (2012).
[3] Kim J.M., Lee G., Kim B.H., Huh Y.S., Lee W., Kim H.J., Ultrasound-assisted synthesis of Li-rich mesoporous $LiMn_2O_4$ nanospheres for enhancing the electrochemical performance in Li-ion batteries, *Ultrasonics Sonochemistry*, **19**, 627–6319, (2012).
[4] Zhang Y., Ouyang L.Z., Chung C.Y., Zhu M., Sputtered Al-doped lithium manganese oxide films for the cathode of lithium ion battery: The post-deposition annealing temperature effect, *J. Alloys Compd*. **480**, 981–986, (2009).
[5] Etacheri V., Marom R., Elazari R., Salitra G., Aurbach D., Challenges in the development of advanced Li-ion batteries: a review, *Energy Environ. Sci*., **4**, 3243–3262, (2011).
[6] Thirunakarana R., Sivashanmugama A., Gopukumar S., Rajalakshmi R., Cerium and zinc: Dual-doped $LiMn_2O_4$ spinels as cathode material for use in lithium rechargeable batteries, *J. Power Sources*, **187**, 565-574, (2009).
[7] Yi T.F. Zhu Y.R., Zhu X.D., Shu J., Yue C.B. & Zhou A.N., A review of recent developments in the surface modification of $LiMn_2O_4$ as cathode material of power lithium-ion battery, *Ionics*, **15**, 779–784, (2009).
[8] Liu X.M., Huang Z.D., Oh S., Ma P.C., Chan P.C.H., Vedam G.K., Kang K., Kim J.K., Sol–gel synthesis of multiwalled carbon nanotube-$LiMn_2O_4$ nanocomposites as cathode materials for Li-ion batteries, *J. Power Sources*, **195**, 4290-4296, (2010).
[9] Arumugam D., Kalaignan G.P., Electrochemical characterizations of surface modified $LiMn_2O_4$ cathode materials for high temperature lithium battery applications, *Thin Solid Films*, **520**, 338–343, (2011).
[10] Jayaprakash N., Sathiyanarayanan K., Kalaiselvi N., A novel approach to explore Zn based anodes for Li-ion battery applications, *Electrochimica Acta*, **52**, 2453-2560, (2007).
[11] Liu H., Cheng C., Zongqiuhu, Zhang K., The effect of ZnO coating on $LiMn_2O_4$ cycle life in high temperature for lithium secondary batteries, *Materials Chemistry and Physics*,**101**, 276-279, (2007).
[12] Wang Y., Wang X., Yang S., Shu H., Wei Q., Wu Q., Bai Y., Hu B., Effect of MgF2 coating on the electrochemical performance of $LiMn_2O_4$ cathode materials, *J. Solid State Electrochem.*, DOI 10.1007/s10008-012-1723-6, (2012).
[13] Tu J., Zhao X. B., Cao G. S., Tu J. P., Zhu T. J., Improved performance of $LiMn_2O_4$ cathode materials for lithium ion batteries by gold coating, *Materials Letters*, **60**, 3251-3254, (2006).